

UC Davis

UC Davis Previously Published Works

Title

Human and Mouse Brown Adipose Tissue Mitochondria Have Comparable UCP1 Function

Permalink

<https://escholarship.org/uc/item/4h67g7wc>

Journal

Cell Metabolism, 24(2)

ISSN

1550-4131

Authors

Porter, Craig
Herndon, David N
Chondronikola, Maria
[et al.](#)

Publication Date

2016-08-01

DOI

10.1016/j.cmet.2016.07.004

Peer reviewed



Published in final edited form as:

Cell Metab. 2016 August 09; 24(2): 246–255. doi:10.1016/j.cmet.2016.07.004.

Human and mouse brown adipose tissue mitochondria have comparable UCP1 function

Craig Porter^{1,6}, David N. Herndon^{1,6}, Maria Chondronikola^{2,6,*}, Tony Chao^{2,6}, Palam Annamalai³, Nisha Bhattarai^{1,6}, Manish Saraf^{1,6}, Karel Capek^{1,6}, Paul T. Reidy², Alexes C. Daquinag⁷, Mikhail G. Kolonin⁷, Blake B. Rasmussen⁴, Elisabet Borsheim^{1,2,**}, Tracy Toliver-Kinsky⁵, and Labros S. Sidossis^{1,6,***}

¹Departments of Surgery, University of Texas Medical Branch

²Rehabilitation Sciences, University of Texas Medical Branch

³Radiology, University of Texas Medical Branch

⁴Nutrition and Metabolism, University of Texas Medical Branch

⁵Anesthesiology, University of Texas Medical Branch

⁶Shriners Hospitals for Children – Galveston

⁷University of Texas Health Science Center Houston

Summary

Brown adipose tissue (BAT) plays an important role in mammalian thermoregulation. The component of BAT mitochondria that permits this function is the inner membrane carrier protein uncoupling protein 1 (UCP1). To the best of our knowledge, no studies have directly quantified UCP1 function in human BAT. Further, whether human and rodent BAT have comparable thermogenic function remains unknown. We employed high-resolution respirometry to determine the respiratory capacity, coupling control, and most importantly, UCP1 function of human

Corresponding author: Craig Porter cr2porte@utmb.edu.

*Affiliation for M. C. is now: Washington University School of Medicine, Lt Louis Missouri

**Affiliation for E. B. is now: Arkansas Children's Nutrition Center, Arkansas Children's Hospital Research Center, University of Arkansas for Medical Sciences.

***Affiliation for L. S. S. is now: Rutgers University, New Brunswick.

Supplemental Information: Supplemental information includes Supplemental Experimental Procedures and Supplemental Figs 1 through 5.

Conflict Of Interest: The authors have no conflicts of interest to disclose.

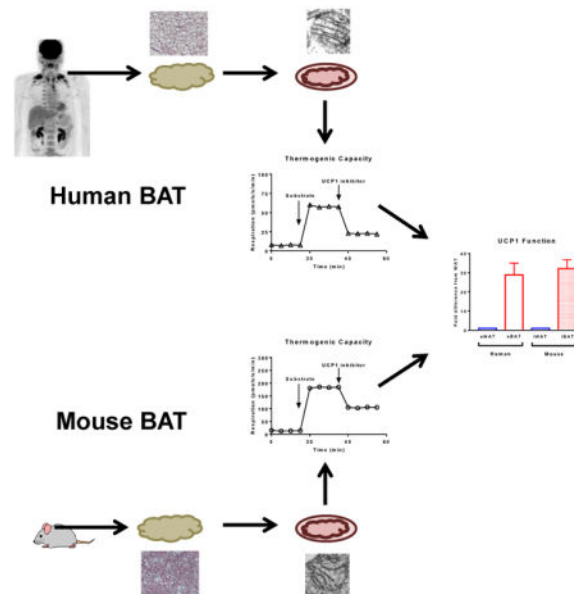
Author Contributions: LSS MC, PA and EB developed the conceptual design of the cold exposure studies. CP and TTK performed all animal study procedures. LSS, MC, PA, TC, NMH, CP, MKS and EB performed cold exposure studies. PA oversaw PET-CT scans and performed biopsies of sBAT and sWAT. PTR and BBR were responsible for recruiting and collecting skeletal muscle biopsies from all healthy participants. DNH and KC were responsible for the care of and collection of adipose tissue from the severely burned patients. CP designed all respirometry experiments and CP, NB and TC performed all respirometry and enzyme activity analysis. MKS performed all electron microscopy and UCP1 gene expression analysis. ACD and MGK performed all immunohistochemistry and immunofluorescence analysis. CP performed statistically analysis, compiled all figures, and is the guarantor of the data. CP drafted the manuscript. All authors reviewed and approved the final version of the manuscript.

Publisher's Disclaimer: This is a PDF file of an unedited manuscript that has been accepted for publication. As a service to our customers we are providing this early version of the manuscript. The manuscript will undergo copyediting, typesetting, and review of the resulting proof before it is published in its final citable form. Please note that during the production process errors may be discovered which could affect the content, and all legal disclaimers that apply to the journal pertain.

supraclavicular BAT and rodent interscapular BAT. Human BAT was sensitive to the purine nucleotide GDP, providing the first direct that human BAT mitochondria have thermogenically functional UCP1. Further, our data demonstrate that human and rodent BAT have similar UCP1 function per mitochondrion. These data indicate that human and rodent BAT are qualitatively similar in terms of UCP1 function.

eTOC PARAGRAPH

Using a PET-CT-guided biopsy technique, Porter et al. provide a detailed analysis of brown adipose tissue (BAT) function and show that human BAT has a respiratory capacity 50-fold greater than white fat. Per mitochondrion, UCP1 function is similar between human and rodent BAT, highlighting the thermogenic potential of human BAT.



Introduction

While BAT is known to play an important physiological role in mammals, including the human neonate, the contemporary view was that humans lost their BAT in early life. The publication of a review article (Nedergaard et al., 2007) and three independent studies demonstrating pronounced glucose disposal in the supraclavicular region of adult humans (Cypess AM, 2009; van Marken Lichtenbelt et al., 2009; Virtanen et al., 2009) led to a paradigm shift in adipocyte biology, where it appeared that adult humans have functional supraclavicular brown adipose tissue (sBAT). These observations (Cypess AM, 2009; van Marken Lichtenbelt et al., 2009; Virtanen et al., 2009) and others (Saito et al., 2009; Zingaretti et al., 2009) rekindled interest in a putative role for sBAT in human energy metabolism.

Given the potential for BAT to alter energy balance in humans, significant efforts have been made to understand the lineage (Jespersen et al., 2013; Shinoda et al., 2015; Wu et al., 2012; Wu et al., 2013), genetic signature (Cypess et al., 2013a; Shinoda et al., 2015; Wu et al.,

2012; Wu et al., 2013; Xue et al., 2015) and thermogenic potential (Cypess et al., 2013a; Shinoda et al., 2015; Vijgen et al., 2013; Xue et al., 2015) of human sBAT. Since UCP1 is the mitochondrial protein responsible for the BAT thermogenesis (Matthias et al., 2000; Nedergaard et al., 1999), measurement of UCP1 function is of critical importance when gauging the physiological significance of human sBAT (Nedergaard and Cannon, 2013; Shabalina et al., 2010). Currently, there are no published data on whether human sBAT has functional UCP1. To address this, we determined mitochondria respiratory capacity and coupling control in sBAT and rodent iBAT. Importantly, we determined UCP1 function per mg of BAT tissue and per mitochondrion in order to characterize mitochondrial function in human sBAT and to compare and contrast this to rodent iBAT.

Results and Discussion

Respiratory capacity and UCP1 function of human and rodent BAT

We employed a PET-CT guided biopsy technique to sample the sBAT depot of humans (Chondronikola et al., 2015) while also sampling abdominal subcutaneous white adipose tissue (sWAT). Mitochondrial respiration was determined in permeabilized sBAT and sWAT from humans and iBAT and inguinal WAT (iWAT) of mice before and after the titration of the UCP1 inhibitor GDP (Supplementary Fig 1). We found that sBAT had a respiratory capacity approximately 50-fold greater than sWAT in human (Fig 1A and 1C). This is in contrast to previous reports that human sBAT has a respiratory capacity ~3-fold (Vijgen et al., 2013) or ~10-fold (Cypess et al., 2013a) greater than sWAT, and studies performed in cultured human white and brown adipocytes (Shinoda et al., 2015; Xue et al., 2015), which suggest that brown adipocyte respiratory capacity is ~2- to 4-fold higher than that of white adipocytes. A likely explanation for the discrepancies in the published data and our current results is the heterogeneity of sBAT, and perhaps our PET-CT guided biopsy technique allowed more precise sampling of sBAT. While the previous studies (Cypess et al., 2013a; Shinoda et al., 2015; Virtanen et al., 2009; Xue et al., 2015) assayed respiratory capacity and/or oligomycin insensitive leak respiration, none directly measured UCP1-dependent respiration. Here, we show marked GDP sensitivity in human sBAT, where UCP1-dependent respiration was significantly greater in sBAT compared to sWAT (28.9 ± 6.1 vs. 0.18 ± 0.07 pmol/s/mg, $P < 0.001$) (Fig 1C). Interestingly, human sBAT exhibited a similar response to GDP when compared to rodent iBAT (Fig 1E and 1F), providing the first biochemical evidence of functional similarity between human and rodent BAT.

Although mass specific leak respiratory capacity (state 2 respiration) was ~3-fold greater in rodent iBAT compared to human sBAT (181.9 ± 15.8 vs. 54.1 ± 11.2 pmol/s/mg) (Fig 1E and 1B), GDP had similar inhibitory effects on rodent iBAT (-45%) and human sBAT (-53%), suggesting qualitatively similar UCP1 function in human and rodent BAT mitochondria. Moreover, the leak control ratio for human sBAT and rodent iBAT were near identical (1.50 ± 0.14 vs. 1.47 ± 0.15) (Supplementary Fig 2A and 2B), further indicating similar UCP1 function in sBAT and iBAT.

The genetic lineage and signature of human supraclavicular brown adipose tissue (sBAT) has been debated. Some suggest that sBAT is analogous to rodent interscapular brown adipose tissue (iBAT) (Cypess et al., 2013b; Lidell et al., 2013; Zingaretti et al., 2009), while others

propose that human sBAT is a *beige* or *brite* fat hybrid (Shinoda et al., 2015; Wu et al., 2012; Wu et al., 2013), exhibiting characteristics of both brown and white adipocytes, while being distinct from rodent iBAT. Further, others suggest that human sBAT may consist of both classical brown adipocytes and *beige/brite* cells (Jespersen et al., 2013). Our current data suggest that from a physiological perspective, human sBAT and rodent iBAT have similar mitochondrial UCP1 function.

Morphology and UCP1 content of human and rodent BAT

As noted above, UCP1-dependent respiration per mg of tissue was greater in rodent iBAT compared to human sBAT (Fig 1 and 1F). The most plausible explanation for this is that in comparison to rodent iBAT, human sBAT exhibits a more heterogeneous cell composition. Morphological examination of human and rodent BAT supports this suggestion, where human sBAT comprises of both large uni-locular and smaller multi-locular cells, whereas rodent iBAT consists of homogeneous multi-locular cells (Fig 2A). Further, electron microscopy indicated that mitochondrial volume density per cell was greater in rodent iBAT compared to human sBAT (Fig 2A), suggesting that rodent iBAT has a greater oxidative capacity than human sBAT. Moreover, the relative intensity of UCP1 staining appeared greater in rodent iBAT in comparison to human sBAT (Fig 2B), which was accompanied by greater mRNA expression of UCP1 (Fig 2C). Thus, per unit of tissue, rodent iBAT contains a more homogeneous population of brown adipocytes containing more mitochondria and UCP1 protein than human sBAT, which likely underlies the greater mass specific respiratory capacity seen in rodent iBAT. The above-mentioned differences may be due to cold-induced iBAT adaptations in mice. While the humans studied here had undergone acute mild cold exposure (~5h at 16°C), mice were housed at ~22°C throughout their lives, which is ~8-10°C below the thermoneutral zone for a mouse (Gordon, 2012). This may explain the species-specific discrepancies in BAT respiratory capacity seen here.

Physiological significance of sBAT in humans

Whether the relatively small (<100g) human BAT have a physiologically significant impact on energy metabolism remains a contentious issue. In the current study, participants had 76±28g of BAT, although this varied significantly (31-186g). As reported elsewhere (Chondronikola et al., 2016a; Chondronikola et al., 2014; Chondronikola et al., 2016b; van Marken Lichtenbelt et al., 2009; Yoneshiro et al., 2011), activation of BAT by a cold exposure protocol increased REE. In this cohort of participants, 5h of non-shivering cold exposure resulted in a 16% increase in REE (281±72 kcal/day) (Fig. 3A). Furthermore, we found that sBAT volume and activity determined by PET-CT strongly correlated with sBAT respiratory capacity and UCP1 function, albeit in a small cohort of humans (Fig. 3B, 3C, 3D and 3E), suggesting that PET-CT represents an indirect measure of BAT mitochondrial function.

Assuming that the increase in REE seen with 5h of mild cold exposure was entirely attributable to BAT, and that this level of activation could be maintained over days and weeks, it would result in the combustion of ~0.87 kg of adipose tissue per month. While we acknowledge that this estimation is speculative at present, if it becomes feasible to chronically activate BAT in humans, at least for several hours per day, this may have a

meaningful impact on energy balance, at least in those individuals with appreciable BAT volume.

Evidence of Symmetrical BAT depots in the neck of humans

Previous work described that the thermogenic potential of human supraclavicular adipose tissue increases when tissue is sampled from deeper compartments of the neck (Cypess et al., 2013a). We collected sWAT from above the platysma muscle and sub-platysmal peri-jugular BAT from both sides of the neck from a patient undergoing surgical reconstruction of burn scars. Grossly, sub-platysmal peri-jugular fat was clearly darker than sWAT harvested from the neck (Fig 4C). On both sides of the neck sub-platysmal peri-jugular sBAT had a leak respiratory capacity 20- to 30- fold greater than sWAT from above the platysma muscle (Fig 4D and 4E). Further, when performing additional mitochondrial respiratory capacity and coupling control assays, we found that sBAT had a large respiratory capacity in the leak state, and that ADP decreased respiration, whereas ADP stimulated respiration in sWAT (Supplemental Fig 3). It should be noted that ADP also stimulates ATP production in sBAT, but the inhibition of UCP1 by ADP results in a net reduction in respiration in sBAT.

Perhaps not surprisingly, we found that the activity of the mitochondrial protein citrate synthase (CS) was significantly greater in these sBAT samples when compared to sWAT for the same patient (Fig 4F), indicating that mitochondrial protein levels are significantly greater in sBAT. Mitochondrial respiration normalized to this proxy of mitochondrial content remained greater in sBAT when compared to sWAT (Fig 4H), suggesting that the gradient in mitochondrial respiratory capacity between human sBAT and sWAT can largely (but not completely) be explained by differences in mitochondrial abundance. Indeed, whether expressed per mg of tissue or per unit of mitochondrial protein, UCP1-dependent respiration was greater in sBAT vs. sWAT of this patient (Fig 4I and Fig 4J).

The above data are generated from samples from one patient. Further, while CS activity is often used as a surrogate of mitochondrial volume density, care should be taken interpreting respiration data to mitochondrial abundance when only one marker is determined. Thus, in matched sWAT and sBAT samples we determined CS (n=5) and cytochrome C oxidase (COX) (n=4) activities. CS activity was 13-fold greater in sBAT vs. sWAT (supplemental Fig 4A), while COX activity was 11-fold greater in sBAT vs. sWAT (supplemental Fig 4D). Thus, whether using a citric acid cycle or electron transport chain enzyme as a proxy of mitochondrial protein abundance, it is apparent that mitochondrial protein levels are significantly greater in human sBAT compared to sWAT. Moreover, we expressed state 2 and UCP1-dependent respiration as functions of CS (supplemental Fig 4B and 5C) and COX (supplemental Fig 4E and 4F) activities. Whether normalized to CS or COX, state 2 respiration was 8-fold greater in sBAT vs. sWAT. Moreover UCP1 dependent respiration was 24-fold and 20-fold greater in sBAT vs. sWAT when normalized to CS or COX, respectively. These data demonstrate that mitochondrial respiratory function is profoundly different in human sBAT compared to sWAT, which is independent of mitochondrial volume density.

Collecting sBAT in any great quantity from a human is not trivial. This is confounded by that fact that sBAT biopsies are rather heterogeneous in nature, often being contaminated by

WAT and connective tissue. With that said, we were able to sample ~100 mg of sBAT from an individual using a PET-CT guided biopsy (Supplemental Fig 5A). Since this tissue appeared reasonably homogenous, we performed biochemical, histological and genetic assays to align morphological and gene expression with measurements of mitochondrial function. In this individual, sBAT respiratory capacity was ~100-fold greater than that of sWAT (Supplemental Fig 5B). Titration of ADP resulted in significant net reduction in respiration in sBAT, again demonstrating significant UCP1 function in sBAT (Supplemental Fig 5B). While sWAT comprised of large unilocular cells, sBAT displayed islands of smaller multi-locular cells, which were immune-reactive for UCP1 (Supplemental Fig 5C). Lastly, transcripts involved in thermogenic function, mitochondrial biogenesis, and fuel metabolism were massively up-regulated in sBAT (Supplemental Fig 5D, 5E, 5F and 5G), suggesting that measurement of UCP1 (mRNA and protein) are related to UCP1 function in human sBAT, at least in this setting.

Human BAT and skeletal muscle have similar respiratory capacity

BAT shares a common lineage with skeletal muscle (Timmons et al., 2007). Interestingly, we found that human sBAT has a mitochondrial respiratory capacity similar to that of skeletal muscle (Fig 5A, 5B, 5E, and 5F). Although skeletal muscle mitochondria exhibit respiratory control in response to ADP, as noted in Supplemental Fig 3 and 5, ADP results in a net inhibition of respiration in sBAT (Fig 5B, 5C and 5F), due to the presence of purine nucleotide sensitive UCP1 in sBAT.

It should be noted that while the net effect of ADP on sBAT is a marked blunting of leak respiration, there is also a concurrent stimulation of respiration linked to ATP production. However, oxidative phosphorylation appears to be minimal in human sBAT mitochondria, as evidenced by a lack of response to the ATP synthase inhibitor oligomycin (Fig 5A, 5B and 5D). Nonetheless, the fact that oligomycin does reduce respiration in human sBAT in the presence of ADP indicates that some ATP production is occurring. This means that the net inhibitory effect of ADP on respiration in sBAT will be under estimated. Since ADP reduced respiration in sBAT by 22.7 ± 8.9 pmol/s/mg whereas oligomycin reduced respiration in sBAT by 3.2 ± 1.0 pmol/s/mg (Fig 5), one may estimate that ADP actually reduced respiration by 25.9 ($22.7 + 3.2$) pmol/s/mg, taking into account ADPs dual effects on respiration in BAT mitochondria.

Unlike skeletal muscle, sBAT mitochondria exhibited little flux control, where leak respiration was almost un-inhibited in sBAT in the presence of substrates (Fig 5G, and 5H). While human sBAT and skeletal muscle have near identical mitochondrial respiratory capacities, mitochondrial respiration is limited by proton accumulation in skeletal muscle, and is only stimulated significantly in the presence of ADP. Human sBAT was not under such respiratory control (Fig 5G, and 5H).

Conclusion

BAT presents a means to alter energy balance and fuel metabolism in humans. The nature of the human sBAT has been studied in detail lately. However, tissue morphology and genetic signatures have been relied upon almost exclusively to determine the thermogenic potential

of human sBAT. Here, we show for the first time that human sBAT has thermogenically functional mitochondria. Further, UCP1 function is similar in human sBAT and rodent iBAT. Thus, these data demonstrate that from a functional perspective, human sBAT is akin to rodent iBAT.

Experimental Procedures

Human Subjects

Human research procedures were approved by the Institutional Review Board at the University of Texas Medical Branch (UTMB). All participants gave informed written consent. Participants (n=5) underwent a 5h mild cold exposure protocol prior to a PET-CT scan to quantify sBAT activity and volume. PET-CT data from n=4 of these participants have been previously published as part of larger cohorts (Chondronikola et al., 2016a; Chondronikola et al., 2014; Chondronikola et al., 2016b). A PET-CT guided biopsy of sBAT and a biopsy of abdominal sWAT were also collected from these participants. sBAT and sWAT was also collected from one severely burned children during a scheduled surgical procedure to release burn scars from the neck region. For information on acute cold exposure, PET-CT imaging and sBAT and sWAT collection and tissue handling, see the Supplemental Information.

Rodent experiments

Animal research procedures were reviewed and approved by the Institutional Animal Care and Use Committee at UTMB. All procedures were performed inline with guidelines set forward by the National Institutes of Health (NIH). Male balb/c mice (8-12 weeks) were housed at ~ 22°C on a 12:12 light dark cycle with free access to drinking water and chow. Animals were sacrificed and iBAT and iWAT samples harvested for analysis. For further information on animal husbandry and iBAT/iWAT sampling and processing, see the Supplemental Information.

Mitochondrial Respirometry

Mitochondrial respiratory rates were determined in fresh permeabilized adipose tissue samples using an O2K respirometer (Oroboros Instruments, Innsbruck, Austria). All measurements were performed in a respiration buffer at 37°C. O₂ concentration was maintained between 200-400 μM in the respiration buffer, which was stirred rigorously by a magnetic stir bar to minimize any O₂ dependency artifacts from the data. Titrations of substrates (pyruvate, octanoyl-l-carnitine, glutamate, malate and succinate) followed by the UCP1 inhibitor GDP were used to directly assay UCP1 function. Further details on respirometric analysis and the respiration protocols used can be found in the Supplemental Information.

Histological analysis

For light and fluorescence microscopy, adipose tissue samples were dehydrated and paraffin embedded prior to sectioning. For electron microscopy, adipose tissue samples were fixed in 2.5% glutaraldehyde. Hematoxylin and eosin and images captured using an Olympus BX41 light microscope (Olympus Corporation, NJ). Ultra-thin sections were examined and images

captured with a JEOL 100CX transmission electron microscope (JEOL USA, Inc., MA). For fluorescence microscopy, confocal images were acquired at 20× with TCS SP5 / LAS AF software (Leica). For detailed information on preparation and processing, see the Supplemental Information.

Gene expression

RNA was extracted from adipose tissue and cDNA was synthesized and amplified. Quantitative real-time PCR analyses were performed on an ABI PRISM 7900HT. For detailed information on preparation and gene expression analysis, see the Supplemental Information.

Citrate synthase activity

Citrate synthase (CS) activity was measured as a surrogate of mitochondrial protein abundance. CS activity was determined spectrophotometrically in adipose tissue lysates as the rate of CoA groups produced by the condensation of acetyl-CoA and oxaloacetate. A detailed description of this assay can be found in the Supplemental Procedures.

Cytochrome C oxidase activity

In addition to CS activity, cytochrome C oxidase (COX) activity was measured as a surrogate of mitochondrial protein abundance. COX activity was determined in adipose tissue lysates using high-resolution respirometry. Briefly, tissue lysates were suspended in respiration buffer containing the Complex III inhibitor Antimycin A. The COX electron donor *N,N,N',N'*-tetramethyl-1,4-benzenediamine dihydrochloride (TMPD) and ascorbate titrated into the respirometer chamber and the peak in O₂ consumption rate was recorded. A detailed description of this assay can be found in the Supplemental Procedures.

Statistical analysis—Values are presented as group means \pm standard error. Group means were compared using a paired t-test. Where multiple comparisons were made, a P-value correction was performed. Statistical significance was accepted when $P < 0.05$. Statistical analysis was performed in GraphPad Prism version 6 (GraphPad Software, Inc., La Jolla, CA).

Supplementary Material

Refer to Web version on PubMed Central for supplementary material.

Acknowledgments

The authors sincerely thank the study participants. We thank Rajesh Kumar of the Department of Nuclear Medicine, UTMB, for performing PET/CT scans. We thank Cynthia Locklin, Carrie Barone, Aikaterini Illiadou, and Ginger Stuart of the Metabolism Unit, Shriners Hospital for Children – Galveston, for their administrative and technical support. We thank Sebastien Labbé, Quebec Heart and Lung Research Institute Centre, Quebec, QC, Canada for assistance in analyzing PET-CT data. We also thank Drs. Shingo Kajimura and Kosaku Shinoda, UCSF Diabetes Center and Department of Cell and Tissue Biology, University of California, San Francisco, for assistance in performing gene analysis.

This work was supported by grants from the NIH (P30 AG024832, RO1 AR049877 and P50 GM060388), American Diabetes Association (1-14-TS-35), Shriners Hospitals for Children (84090, 85310 and 84510) and the Department of Surgery at UTMB. Study visits were conducted with the support of the Institute for Translational

Sciences at UTMB, which is supported by a Clinical and Translational Science Award (UL1TR000071) from the National Center of Advancing Translational Sciences, National Institutes of Health. CP was supported by a training grant (H133P110012) from the National Institute for Disabilities and Rehabilitation Research and the Department of Education.

References

- Chondronikola M, Annamalai P, Chao T, Porter C, Saraf M, Cesani F, Sidossis L. A percutaneous needle biopsy technique for sampling the supraclavicular brown adipose tissue depot of humans. *Int J Obes (Lond)*. 2015 Epub ahead of print.
- Chondronikola M, Volpi E, Børsheim E, Chao T, Porter C, Annamalai P, Yfanti C, Labbe S, Hurren N, Malagaris I, et al. Brown Adipose Tissue Is Linked to a Distinct Thermoregulatory Response to Mild Cold in People. *Front Physiol*. 2016a; 19:7, 129.
- Chondronikola M, Volpi E, Børsheim E, Porter C, Annamalai P, Enerbäk S, Liddell ME, Saraf M, Labbe S, Hurren S, et al. Brown adipose tissue activation improves glucose homeostasis and insulin sensitivity in humans. *Diabetes*. 2014; 63:4089–4099. [PubMed: 25056438]
- Chondronikola M, Volpi E, Børsheim E, Porter C, Saraf M, Annamalai P, Yfanti C, Chao T, Wong D, Shinoda K, et al. Brown Adipose Tissue Activation Is Linked to Distinct Systemic Effects on Lipid Metabolism in Humans. *Cell Metab*. 2016b; 23(6):1200–1206. [PubMed: 27238638]
- Cypess A, White A, Vernochet C, Schulz T, Xue R, Sass C, Huang T, Roberts-Toler C, Weiner L, Sze C, et al. Anatomical localization, gene expression profiling and functional characterization of adult human neck brown fat. *Nat Med*. 2013a; 19
- Cypess A, White A, Vernochet C, Schulz T, Xue R, Sass C, Huang T, Roberts-Toler C, Weiner L, Sze C, et al. Anatomical localization, gene expression profiling and functional characterization of adult human neck brown fat. *Nat Med*. 2013b; 19:635–639. [PubMed: 23603815]
- Cypess AM, L S, Williams G, Tal I, Rodman D, Goldfine AB, Kuo FC, Palmer EL, Tseng YH, Doria A, Kolodny GM, Kahn CR. Identification and importance of brown adipose tissue in adult humans. *N Engl J Med*. 2009; 360:1509–1517. [PubMed: 19357406]
- Gordon C. Thermal physiology of laboratory mice: Defining thermoneutrality. *J Therm Biol*. 2012; 37:654–685.
- Jespersen N, Larsen T, Peijs L, Dugaard S, Homøe P, Loft A, de Jong J, Mathur N, Cannon B, Nedergaard J, et al. A classical brown adipose tissue mRNA signature partly overlaps with brite in the supraclavicular region of adult humans. *Cell Metab*. 2013; 17:798–805. [PubMed: 23663743]
- Lidell M, Betz M, Dahlqvist Leinhard O, Heglind M, Elander L, Slawik M, Mussack T, Nilsson D, Romu T, Nuutila P, et al. Evidence for two types of brown adipose tissue in humans. *Nat Med*. 2013; 19:631–634. [PubMed: 23603813]
- Matthias A, Ohlson K, Fredriksson J, Jacobsson A, Nedergaard J, Cannon B. Thermogenic Responses in brown fat cells are fully UCP1-dependent. *Journal of Biological Chemistry*. 2000; 275:25073–25081. [PubMed: 10825155]
- Nedergaard J, Bengtsson T, Cannon B. Unexpected evidence for active brown adipose tissue in adult humans. *Am J Physiol Endocrinol Metab*. 2007; 293:444–452.
- Nedergaard J, Cannon B. UCP1 mRNA does not produce heat. *Biochim Biophys Acta*. 2013
- Nedergaard J, Matthias A, Golozoubova V, Jacobsson A, Cannon B. UCP1: the original uncoupling protein--and perhaps the only one? New perspectives on UCP1, UCP2, and UCP3 in the light of the bioenergetics of the UCP1-ablated mice. *J Bioenerg Biomembr*. 1999; 31:475–491. [PubMed: 10653476]
- Saito M, Okamatsu-Ogura Y, Matsushita M, Watanabe K, Yoneshiro T, Nio-Kobayashi J, Iwanaga T, Miyagawa M, Kameya T, Nakada K, et al. High incidence of metabolically active brown adipose tissue in healthy adult humans: effects of cold exposure and adiposity. *Diabetes*. 2009; 58:1526–1531. [PubMed: 19401428]
- Shabalina I, Ost M, Petrovic N, Vrbacky M, Nedergaard J, Cannon B. Uncoupling protein-1 is not leaky. *Biochim Biophys Acta*. 2010; 1797:773–784. [PubMed: 20399195]
- Shinoda K, Luijten I, Hasegawa Y, Hong H, Sonne S, Kim M, Xue R, Chondronikola M, Cypess A, Tseng Y, et al. Genetic and functional characterization of clonally derived adult human brown adipocytes. *Nat Med*. 2015; 21:389–394. [PubMed: 25774848]

- Timmons J, Wennmalm K, Larsson O, Walden T, Lassmann T, Petrovic N, Hamilton D, Gimeno R, Wahlestedt C, Baar K, et al. Myogenic gene expression signature establishes that brown and white adipocytes originate from distinct cell lineages. *Proc Natl Acad Sci U S A*. 2007; 104:4401–4406. [PubMed: 17360536]
- van Marken Lichtenbelt W, Vanhomerig J, Smulders N, Drossaerts J, Kemerink G, Bouvy N, Schrauwen P, Teule G. Cold-activated brown adipose tissue in healthy men. *N Engl J Med*. 2009; 360:1500–1508. [PubMed: 19357405]
- Vijgen G, Sparks L, Bouvy N, Schaart G, Hoeks J, van Marken Lichtenbelt W, Schrauwen P. Increased oxygen consumption in human adipose tissue from the “brown adipose tissue” region. *J Clin Endocrinol Metab*. 2013; 98:1230–1234.
- Virtanen K, Lidell M, Orava J, Heglind M, Westergren R, Niemi T, Taittonen M, Laine J, Savisto N, Enerbäck S, et al. Functional brown adipose tissue in healthy adults. *N Engl J Med*. 2009; 360:1518–1525. [PubMed: 19357407]
- Wu J, Boström P, Sparks L, Ye L, Choi J, Giang A, Khandekar M, Virtanen K, Nuutila P, Schaart G, et al. Beige adipocytes are a distinct type of thermogenic fat cell in mouse and human. *Cell*. 2012; 150:366–376. [PubMed: 22796012]
- Wu J, Cohen P, Spiegelman B. Adaptive thermogenesis in adipocytes: is beige the new brown? *Genes Dev*. 2013; 27:234–250. [PubMed: 23388824]
- Xue R, Lynes M, Dreyfuss J, Shamsi F, Schulz T, Zhang H, Huang T, Townsend K, Li Y, Takahashi H, et al. Clonal analyses and gene profiling identify genetic biomarkers of the thermogenic potential of human brown and white preadipocytes. *Nat Med*. 2015; 21:760–768. [PubMed: 26076036]
- Yoneshiro T, Aita S, Matsushita M, Kameya T, Nakada K, Kawai Y, Saito M. Brown adipose tissue, whole-body energy expenditure, and thermogenesis in healthy adult men. *Obesity*. 2011; 19:13–16. [PubMed: 20448535]
- Zingaretti M, Crosta F, Vitali A, Guerrieri M, Frontini A, Cannon B, Nedergaard J, Cinti S. The presence of UCP1 demonstrates that metabolically active adipose tissue in the neck of adult humans truly represents brown adipose tissue. *FASEB J*. 2009;3113–3120. [PubMed: 19417078]

Highlights

- Human BAT has a respiratory capacity 50- to 100-fold greater than that of WAT.
- Human BAT has functional UCP1.
- Per mitochondrion, UCP1 function is similar in human and rodent BAT.
- BAT and skeletal muscle have similar respiratory capacities in humans.

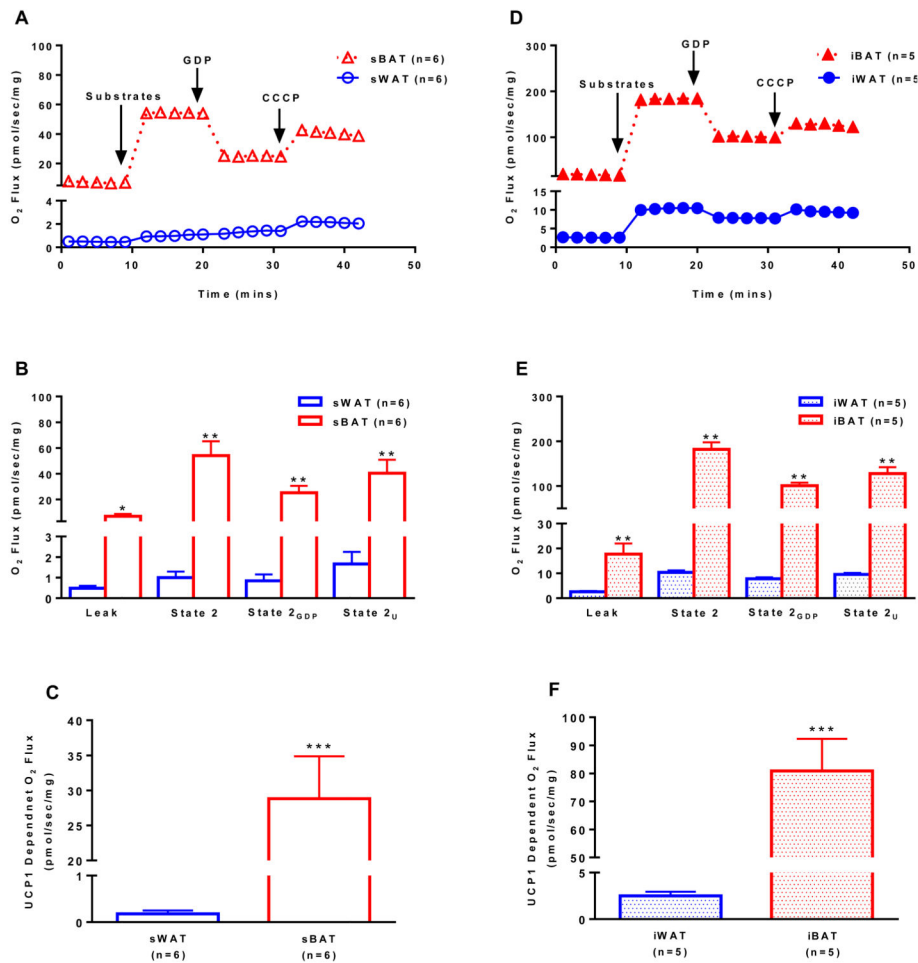


Figure 1. Mitochondrial respirometry in human and rodent white and brown adipose tissue. **(a)** Representative respiration experiments performed on permeabilized sWAT and sBAT from humans following the sequential titration of substrates (1.5 mM octanoyl-l-carnitine, 5 mM pyruvate, 2 mM malate, 10 mM glutamate), 20 mM of the UCP1 inhibitor GDP and 5 μ M of the protonophore CCCP (values are group means). **(b)** Comparison of respiratory states (state 2, State 2_{GDP}, and State 2_U) for human sWAT and sBAT shown in panel **a**. **(c)** UCP1-dependent respiration in human sWAT and sBAT calculated as the change in respiration following titration of the UCP1 inhibitor GDP. **(d)** Representative respiration experiments performed on permeabilized iWAT and iBAT from mice as described in panel **a**. **(e)** Comparison of respiratory states (state 2, State 2_{GDP}, and State 2_U) for mouse iWAT and iBAT shown in panel **d**. **(f)** UCP1-dependent respiration in mouse iWAT and iBAT calculated as in **c**. Note that leak respiration prior to titration of substrates is supported by endogenous substrates, likely FFAs. Values are presented as group means \pm SEM unless otherwise stated. * $P < 0.05$, ** $P < 0.01$, and *** $P < 0.001$ vs. WAT.

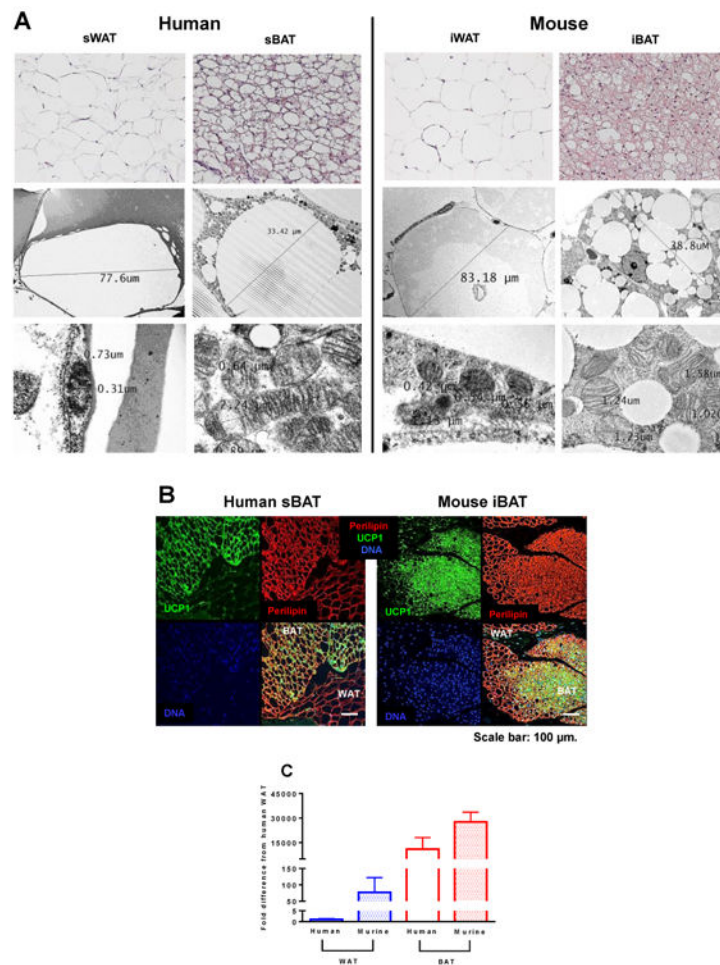


Figure 2. Morphological and molecular evaluation of human and rodent white and brown adipose tissue. **(a)** Representative hematoxylin and eosin stained sections of human sWAT and sBAT and rodent iWAT and iBAT (top row) showing differences in cell size and morphology between brown and white adipocytes from both humans and mice. Electron micrograph imaging humans WAT and sBAT and rodent iWAT and iBAT (middle row). Electron micrograph imaging of mitochondrial abundance and morphology of human sWAT and sBAT and rodent iWAT and iBAT (bottom row), showing the scarcity of mitochondrion in white adipose tissue in contrast to an abundance of large electron-dense organelles in brown adipose tissue. **(b)** Immunofluorescence staining of human sBAT and rodent iBAT for UCP1 (green), perilipin (red), and nuclei (blue) underscoring morphological differences between adipose tissue types and the presence of UCP1 in brown adipocytes. **(c)** UCP1 mRNA expression in human and rodent white and brown adipose tissue. Values are means \pm SEM.

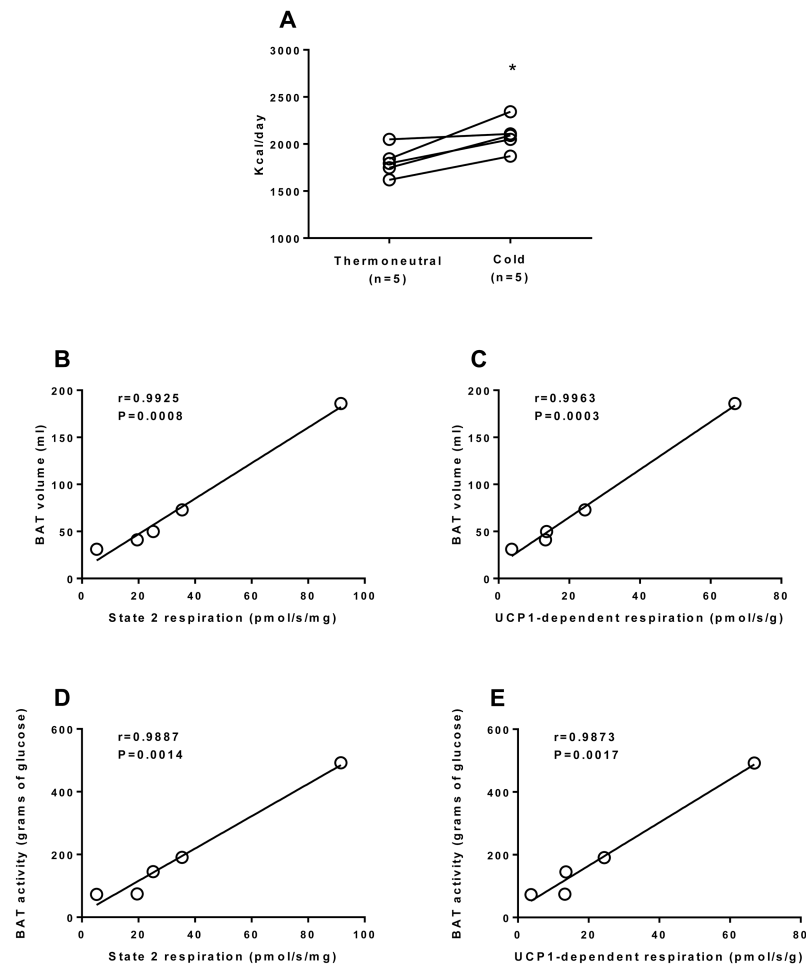


Figure 3.

The metabolic significance of human brown adipose tissue. **(a)** Resting energy expenditure (REE) determined during thermoneutral conditions and mild non-shivering cold exposure in 5 healthy men. There was a significant (~16%) increase in REE with mild non-shivering cold exposure (* $P < 0.05$), likely the result of acute BAT activation. BAT volume (ml) determined by PET-CT significantly correlated with BAT mitochondrial respiratory capacity **(b)** and UCP1 function **(c)** in humans. BAT activity (total BAT glucose disposal) determined by PET-CT significantly correlated with BAT mitochondrial respiratory capacity **(d)** and UCP1 function **(e)** in humans. These data suggest that indices of BAT metabolic function *in vivo* are related to sBAT mitochondrial respiratory capacity and UCP1 function, although we acknowledge that the sample size is limit ($n=5$). It should be noted that there was also a strong correlation ($r=0.998$, $P < 0.001$) between state 2 and UCP1-dependent respiration (data not shown), suggesting a relationship between BAT mitochondrial respiratory capacity and UCP1 function.

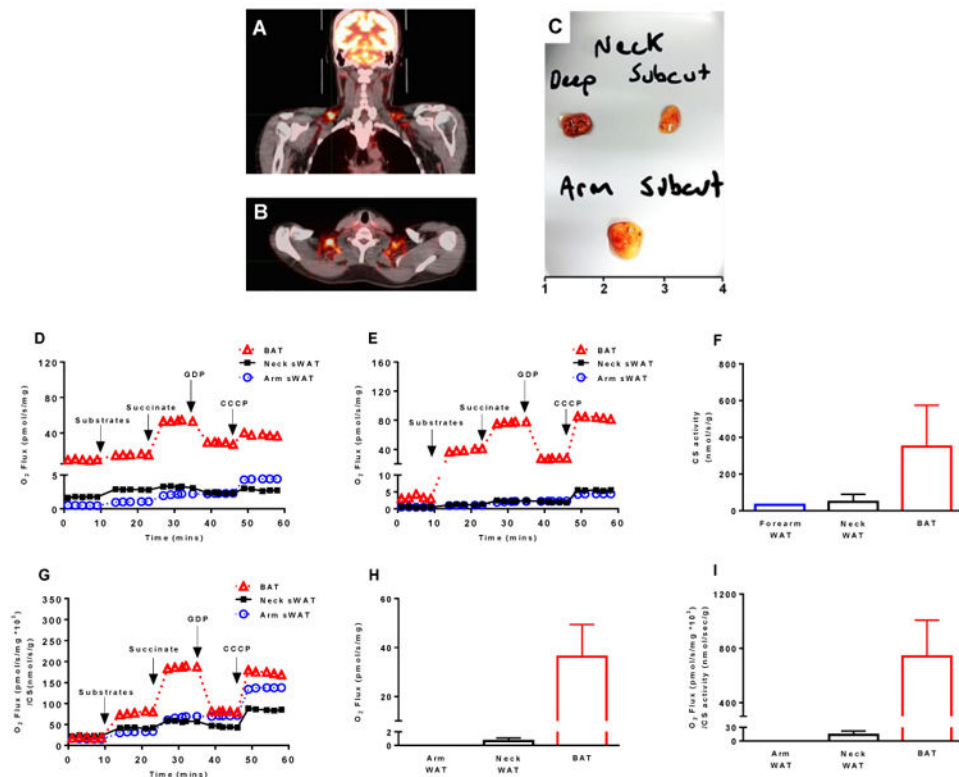


Figure 4.

Functional evidence of symmetrical brown adipose tissue depots in humans. (a & b) PET-CT imaging showing that humans have symmetrical sBAT depots. (c) Sub-platysmal peri-jugular adipose tissue was sampled from both the left and right side of the neck of a severely burned individual. sWAT was sampled from the left and right sides of the neck above the platysma muscle, and forearm sWAT was also sampled from this patient. Panel c depicts the gross form and coloration of these three adipose tissue types, where deep neck fat depicts sub-platysmal peri-jugular adipose tissue and subcut neck depicts sWAT harvested above the platysma. (d) BAT and sWAT respirometry from the left side of the neck and sWAT from the forearm. (e) BAT and sWAT respirometry from the right side of the neck from the same patient shown in panel d (data from the same forearm sWAT sample shown in panel d is included for comparison). These data suggest that sBAT on either side of the neck contain mitochondria with functional UCP1. (f) Quantification of citrate synthase (CS) activity (a proxy of mitochondrial protein abundance) in sWAT from the forearm (n=1 sample), sWAT from the left and right side of the neck (n=2 samples), and BAT from both the left and right side of the neck (n=2 samples). (g) Mitochondrial respiration data presented in panels d and e normalized to CS activity data presented in panel f suggests that much (but not all) of the gradient in oxidative capacity between human WAT and BAT may be explained by mitochondrial protein abundance. (h) Mass specific UCP1-dependent respiration (respiration per mg of tissue) in neck BAT and sWAT and forearm sWAT. (i) Mitochondria specific UCP1-dependent respiration (respiration per unit of CS activity) in neck BAT and sWAT and forearm sWAT. These results suggest that whether presented per unit of tissue or

mitochondrial protein, UCP1 function is only apparent in sBAT of humans. Note that leak respiration prior to titration of substrates is supported by endogenous substrates, likely FFAs.

Author Manuscript

Author Manuscript

Author Manuscript

Author Manuscript

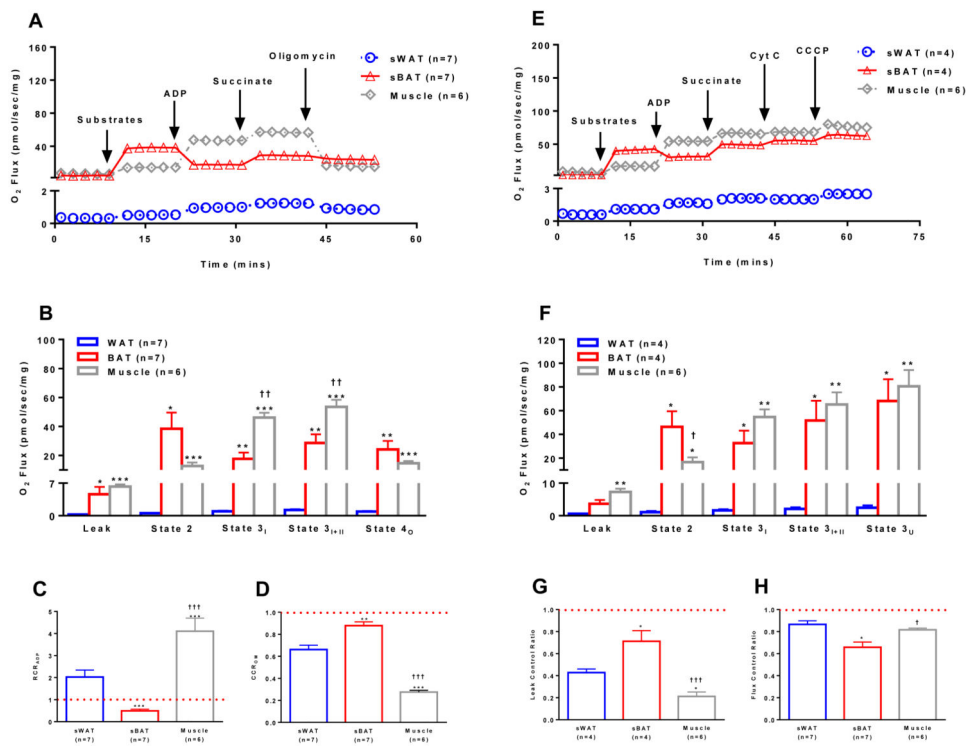


Figure 5.

Comparison of mitochondrial respiratory capacity and coupling control in human sWAT, sBAT, and skeletal muscle. **(a)** Representative respiration experiments performed on permeabilized sWAT and sBAT from the same seven individuals and skeletal muscle from six separate individuals following the sequential titration of substrates and oligomycin as describe in Fig 1A (values are group means). **(b)** Comparison of respiratory states for sWAT, sBAT and skeletal muscle shown in panel **a** highlight similar respiratory capacity in human BAT and skeletal muscle. **(c)** The respiratory control ratio for ADP (RCR_{ADP}) calculated by dividing state 3_I by state 2. A $RCR_{ADP} < 1$ indicates that mitochondria are not coupled in human sBAT. **(d)** The coupling control ratio for oligomycin (CCR_{OM}) calculated by dividing state 4_O by state 3_{I+II} . A $CCR_{OM} = 1$ indicates that mitochondria are insensitive to oligomycin and thus are uncoupled. A lower CCR_{OM} suggest better coupled mitochondria in sWAT and skeletal muscle. **(e)** Representative respiration experiments performed on permeabilized sWAT, sBAT and skeletal muscle from the same individuals in panel **a** following the sequential titration of substrates (1.5 mM octanoyl-l-carnitine, 5 mM pyruvate, 2 mM malate, and 10 mM glutamate), ADP (5 mM), succinate (10 mM), cytochrome C (10 μ M) and the ionophore CCCP (5 μ M) (values are group means). **(f)** Comparison of respiratory states for sWAT, sBAT and skeletal muscle shown in panel **e** again showing that sBAT has a respiratory capacity more akin to that of muscle than sWAT in humans. **(g)** The leak control ratio (LCR), calculated by dividing state 3_{I+II} by state 3_U , shows the absence of leak control in human sBAT. The lux control ratio (FCR), an index of the efficiency of the oxidative phosphorylation system, was calculated by dividing state 2 by state 3_U . A lower FCR in BAT demonstrates poor mitochondrial coupling control. Note that while the addition of ADP to sBAT reduces leak respiration there is also likely a stimulation of coupled

respiration (ATP production). However, this is minimal given the blunted response to the ATP synthase inhibitor oligomycin observed in coupled sBAT mitochondria. Note that leak respiration prior to titration of substrates is supported by endogenous substrates, likely FFAs. Values are presented as means \pm SE unless otherwise stated. *P<0.05 vs. sWAT; **P<0.01 vs. sWAT; ***P<0.001 vs. sWAT; †P<0.05 vs. sBAT; ††P<0.01 vs. sBAT; †††P<0.001 vs. sBAT.

Author Manuscript

Author Manuscript

Author Manuscript

Author Manuscript